Wideband Characterization of UHF RFID Channels for Ranging and Positioning

Daniel Arnitz†, Ulrich Muehlmann‡, and Klaus Witrisal†

† Signal Processing and Speech Communication Laboratory, Graz University of Technology, Graz, Austria
{daniel.arnitz, witrisal}@tugraz.at
‡ NXP Semiconductors, Gratkorn, Austria
ulrich.muehlmann@nxp.com

***Abstract*—Positioning is a much-desired feature in today's passive UHF RFID systems and thus a central topic of research: various positioning methods for passive backscattering have been presented in the past years. Even though multipath propagation is the most prominent source of error for all these systems, the UHF RFID channel is not well-understood in this respect. This work presents the first wideband characterization of typical UHF RFID channels (indoor, short-range, large TX antennas, ...) based on measurements and shows that the ranging error massively depends on these parameters.**

I. Introduction, Motivation, and Relevance

Several narrowband methods for UHF RFID positioning using the phase shifts between multiple carriers have been published during the last years, f.i., [1], [2]. The most prominent benefit of these systems compared to ultrawideband (UWB) positioning is their ability to work with currently used tags and to fit into existing spectral masks with only minimal changes to regulations.

For such multicarrier systems, phase shifts between the carriers, neglecting everything except the propagation channel, contain two components: One component is created by the wave propagation along the shortest path between transmitter and receiver (line-of-sight, LOS, path), and the other one is created by multipath propagation.

Increasing the frequency separation between the carriers increases the spatial resolution of the distance estimate for a given phase resolution and decreases the influence of noise, but invariably increases the error created by multipath propagation. Carriers with a spacing outside the coherence bandwidth of the channel will experience independent fading, rendering the phases close to being uniform between $-\pi$ and π (Rayleigh fading). As a consequence, all range information is lost and any ranging or positioning method using such phase differences will fail. A more thorough analysis can be found in [2].

Even though, for the above reasons, multipath propagation is the most prominent source of error in UHF RFID ranging and positioning, the underlying channel characteristics are not well-understood for typical UHF RFID channels (indoor, short-range, large TX antenna arrays,...). This work presents an (ultra)wideband channel characterization for typical UHF RFID setups and shows that neglecting multipath propagation is not feasible for indoor scenarios.

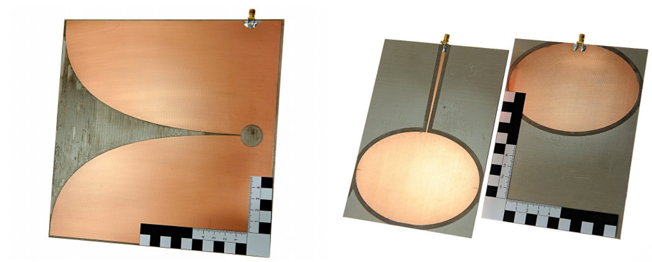

Fig. 1. Custom design antennas used for measurements (left: TX, right: RX).

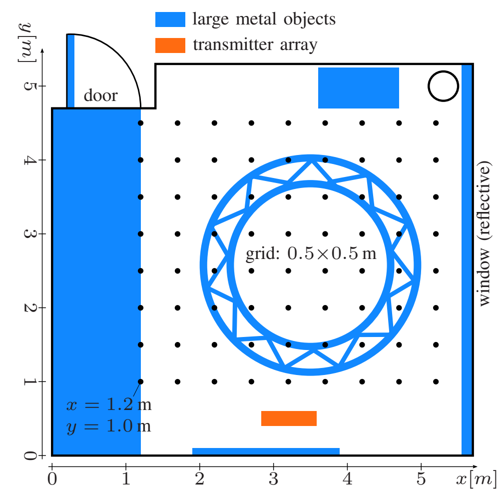

Fig. 2. Environment plan (simplified) with TX and RX positions.

II. Measurement Setup and Environment

The used measurement setup consists of a $4{\times}1$ transmitter (TX) antenna array ($60{\times}21{\times}21$ cm) resembling the gain pattern of typical UHF RFID gate antennas (main lobe: $\pm 20^\circ$ horz., $\pm 60^\circ$ vert.) and omnidirectional receiver (RX) antennas with a gain pattern resembling that of RFID tags; cf. Fig. 1. Measurements were taken in the range of 500 through 1500 MHz using a vector network analyzer. The presented measurements were performed in the semi-industrial environment shown in Fig 2: Walls, floor, and ceiling are made of concrete, and the window is reflective (metal coating). The room contains large metal objects, such as metal platings and conduits, and a complex metal cabinet. Also a large circular

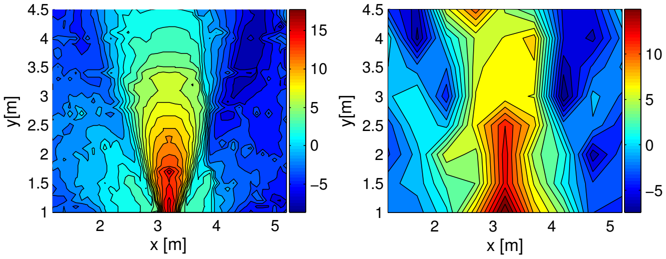

Fig. 3. K-Factor w.r.t. the LOS-component in dB (left: sim, right: meas).

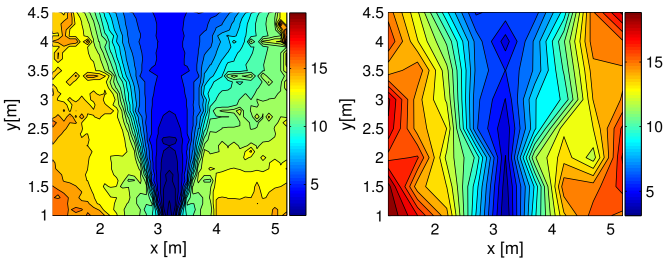

Fig. 4. RMS delay spread in ns (left: simulation, right: measurement).

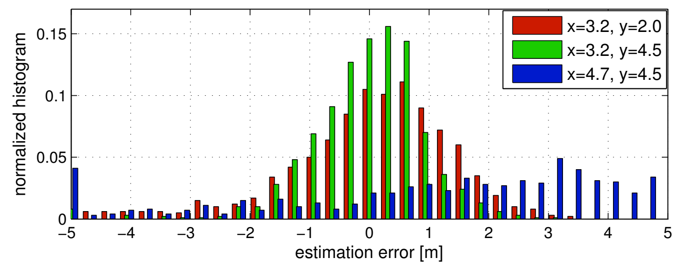

Fig. 5. Ranging error distr. for a two-carrier system, spacing 1 MHz, centers at 0.5..1.5 GHz, for three positions (two inside, one outside main lobe).

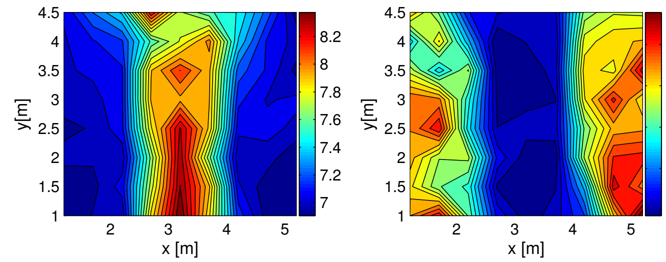

Fig. 6. Measured 70 % coherence bandwidth in Hz (powers of 10; left) and ranging error in meters for 1000 carriers to show the NLOS bias (right).

aluminum strut is mounted on the ceiling.

III. Channel Model and Simulation Setup

Simulation results have been created by [3] with some enhancements, such as simple ray-tracing abilities. The simulation includes RX-antenna and TX-array directivities (far field patterns), reflections at walls, floor, and ceiling (simple raytracing), and a statistical model for scattered components [4]. Not modeled are exact geometries, material properties except for the refraction index, and near-field effects such as the TX antenna array size.

The channel model consists of a deterministic largescale part (log-distance LOS path), a deterministic smallscale part (reflections), as well as a stochastic smallscale part (scattered components).

IV. Measurement and Simulation Results

Plots of the two most important channel parameters for narrow- and wideband ranging, namely the K-factor w.r.t. the power fraction in the LOS component and the RMS delay spread, can be found in Figs. 3 and 4 along with their respective simulation results. Differences between simulation and measurement can mostly be related to near field effects (bottom close to TX) and to local distortions caused by metal objects (top, right).

The K-factor within the main lobe is surprisingly low, given that the TX→RX separation is just a few meters an the high directivity of the TX array. Outside the main lobe, the LOS component is typically weaker than the strongest reflected path and always weaker than the sum of reflected paths. This makes multicarrier-based ranging more than challenging: Fig. 5 shows the ranging error distribution for three representative positions (two inside the main lobe, one outside) when using two carriers with 1 MHz spacing in the range of 0.5 through 1.5 GHz. Note that, for very short distances, near field effects result in an increasing standard deviation and a biased estimate.

Fig. 6 finally compares the coherence bandwidth of the channel to a theoretical lower bound limit for straightforward narrowband ranging, combining 1000 carriers (overall bandwidth 1 GHz). As can be seen, the estimate is biased outside the main lobe due to the weak LOS path and multiple reflections.

V. Conclusion

Wideband channel parameters for a UHF RFID indoor scenario were derived from measurements and compared to simulation results. Based on these measurements, errors for multicarrier positioning systems have been presented and compared to wideband channel parameters. We've shown that positioning methods without taking the wideband channel into account will fail under realistic indoor conditions. Future work will include different scenarios, such as gate applications.

VI. Acknowledgments

The authors would like to express their gratitude to Grzegorz Adamiuk from University of Karlsruhe for the antenna designs.

This work was supported by NXP Semiconductors, Gratkorn, Austria, and by the Austrian Research Promotion Agency (FFG) under grant 818072. The measurements were taken using remote control functions developed by Carlos Manuel Delgado Ramirez during his master's thesis at TU Graz.

REFERENCES

[1] X. Li, Y. Zhang, and M. G. Amin, "Multifrequency-based range estimation of RFID tags," in *Proc. IEEE Intl. Conf. on RFID, RFID'09*, Orlando, Florida, Apr. 2009, pp. 28–33.

[2] D. Arnitz, K. Witrisal, and U. Muehlmann, "Multi-frequency continuous-wave radar approach to ranging in passive UHF RFID," *IEEE Trans. Microw. Theory Tech.*, vol. 57, no. 5, pp. 1398–1405, Jul. 2009.

[3] D. Arnitz, U. Muehlmann, T. Gigl, and K. Witrisal, "Wideband system-level simulator for passive UHF RFID," in *Proc. IEEE Intl. Conf. on RFID, RFID'09*, Orlando, Florida, Apr. 2009.

[4] K. Witrisal, Y.-H. Kim, and R. Prasad, "A new method to measure parameters of frequency-selective radio channels using power measurements," *IEEE Trans. Commun.*, vol. 49, no. 10, pp. 1788–1800, Oct. 2001, 10.1109/26.957401.